arXiv:cond-mat/0207149v1 [cond-mat.str-el] 5 Jul 2002

Vacuum polarization in nanotubes

K. Sasaki[1], A. A. Farajian[2], H. Mizuseki[2], and Y. Kawazoe[2]
[1] *Department of Physics, Tohoku University, Sendai 980-8578, Japan*
[2] *Institute for Materials Research, Tohoku University, Sendai 980-8577, Japan*
(Dated: December 2, 2024)

The vacuum polarization in various types of carbon nanotubes is theoretically investigated in a model describing the π-electrons with the Coulomb interaction. It is pointed out that screened Coulomb interactions between massive fermions in metallic nanotubes weaken drastically as compared with the one in semi-conducting nanotubes. It is also shown that the Friedel oscillation around an external charge is absent in un-doped armchair nanotubes due to a constraint on the momentum phase space of the π-electrons.

I. INTRODUCTION

Quantum mechanical behavior of the π-electrons in carbon nanotubes(CNTs [1, 2, 3]) is governed by many kinds of interactions [4, 5, 6, 7]. Among others the Coulomb interaction between electrons is the most important interaction and drives the system into a strongly correlated state [5, 6, 7]. Several aspects of the Coulomb interaction are already seen in some experiments of charging [8] and of temperature dependent resistivity [9] which are consistent with current understanding of low energy excitations in metallic CNTs. The low energy excitations in the metallic CNTs are theoretically modeled by *massless* bands (linear dispersion bands) with the Coulomb interaction as Tomonaga-Luttinger liquid [5, 6, 7]. However when we consider, for example, a localized perturbation, it is not clear if the low energy theories describe the physics correctly. Because short distance physics corresponds to high energy, *massive* bands (other sub-bands except the massless bands) would come into dynamics. In this article, we focus on the effect of the π-electrons on the Coulomb interaction, namely, vacuum polarization.

It is important to study the massive bands effect because of the geometrical structure of CNTs. Roughly speaking, the strength of one-dimensional long-range Coulomb interaction is inversely proportional to diameter of nanotube; besides, gap energy of the massive bands also scaled as inverse of the diameter. Therefore effect of the massive bands on the massless bands is universal for all kind of nanotube. Furthermore the number of the massive bands increase as the diameter of the nanotube increase. So, for the case of CNT with large diameter or the case of multi-walled CNTs, the quantum correction to the low energy dynamics due to the massive bands would be significant. It is the purpose of the present work to construct a field theoretical model for the π-electrons and investigate the vacuum polarization. We apply the result to an analysis of the screening of an external charge in the metallic CNTs.

As for the screening, the high-energy massive mode excitations can in principle affect the screening phenomena through two different mechanisms; adding massive-fermions loop corrections to the interactions of massless bands and direct interaction of massive bands (non-perturbative effect of the massive bands on the screening phenomena). We will focus on the former mechanism. To investigate the later mechanism, a lattice field theoretical model employing a fully self-consistent tight-binding approach including the Coulomb interaction [10, 11] would be suitable.

The paper is composed as follows. A model Hamiltonian for the π-electrons is constructed in Sec. II. In Sec. III, we quantize the π-electron fields and define propagator for each field. Then we calculate the vacuum polarization amplitude in Sec. IV and discuss the application to the screening of an external localized charge. Summary and conclusion are given in Sec. V.

II. MODEL CONSTRUCTION

We construct a continuous field theoretical model describing the π-electrons of CNTs in this section. To do this, let us begin with an electron wave function on the graphite sheet. The wave function is two components because of the honeycomb lattice structure of the graphite sheet [12],

$$\Psi_s = \begin{pmatrix} \Psi_{\bullet s} \\ \Psi_{\circ s} \end{pmatrix}, \tag{1}$$

where $s \in \{\uparrow, \downarrow\}$ is the electron spin index. A CNT can be thought of as a layer of graphite sheet fold up into a cylinder. Thus, the periodic boundary condition along the circumference of the tube forces the wave vector into discrete vectors. As a result, the electron wave function in the tube is expanded by two-component wave functions which have a discrete wave vector as,

$$\Psi_s(r) = \sum_N \psi_{Ns}(r), \tag{2}$$

where $N \in \{0, 1, \cdots\}$ is a label for the discrete wave vector and $r = (x, y)$ are the coordinates on the surface of the nanotube. A field theory describing the dynamics of the π-electrons in CNTs consists of the two-component fermion fields ψ_{Ns} interacting with each other via the Coulomb interaction.

Energy dispersion relation of each fermion field specifies a band structure. The band structure depends on geometry of a CNT, therefore the definition of fields also depends on it. There are two kinds of geometry which one refer to metallic CNTs that have linear dispersions near the Fermi points. They are contrasted with semiconducting CNTs which involve no linear dispersion near the Fermi level. The Hamiltonian density modeling these systems is given by $\mathcal{H} = \mathcal{H}_F + \mathcal{H}_C$ where $\mathcal{H}_F$ is the free (unperturbed) part and $\mathcal{H}_C$ is the perturbed part including the Coulomb interaction.

A. Kinetic term

Suppose we include only tight-binding interactions, then the kinetic Hamiltonian density is given by $\mathcal{H}_F = \sum_{Ns} \mathcal{H}_N$ where

$$\begin{aligned} \mathcal{H}_N &= \psi^\dagger_{Ns} h_N \psi_{Ns} \\ &= \psi^\dagger_{Ns} V_\pi \begin{pmatrix} 0 & z(k^N_x, \hat{k}_y) \\ z^*(k^N_x, \hat{k}_y) & 0 \end{pmatrix} \psi_{Ns}. \end{aligned} \quad (3)$$

V_π is the hopping integral, $\hat{k}_y = -i\partial_y$ is the wave vector along tubule axis. The discrete wave vector around the circumference is

$$ak^N_x = -\frac{4\pi}{3\sqrt{3}} + \frac{2a}{d}N, \quad (4)$$

where N is a positive integer, d is the diameter of a CNT and $a = 1.42[\mathring{A}]$ the lattice spacing. Here we consider the case of metallic zigzag CNTs. The function $z(k_x, k_y)$ indicates the hopping amplitude between sub-lattices (or the components) and is defined as

$$z(k_x, k_y) = \sum_i e^{ik\cdot u_i}, \quad (5)$$

where the vector u_i is a triad of vectors pointing in the direction of the nearest neighbors of a carbon site [12].

The free Hamiltonian densities whose wave vector is equal to $ak^N_x = -\frac{4\pi}{3\sqrt{3}}$ or $\frac{4\pi}{3\sqrt{3}}$ describe massless fermions (electrons and holes in the massless bands) and the others are for massive fermions in the metallic zigzag CNTs. The massless fermions are analyzed by means of the current algebra or by a framework of TL liquid [5, 6, 7]. We illustrate the band structure of a metallic zigzag CNT for later convenience in Fig. 1. In the case of the zigzag CNTs, the diameter is given by the following formula

$$d = \frac{3\sqrt{3}a}{2\pi}N_0, \quad (6)$$

where N_0 is the number of the hexagon along the circumference. If there are six hexagons, the diameter is about $(d =)7.04[\mathring{A}]$. The number of the bands is given by $3N_0$ which gives us the correct number of the π-electrons of the system. Note that ak^N_x and $ak^{N+\frac{3}{2}N_0}_x$ have the same physical momentum around the axis because of congruent vectors. For example, $N = 0, 12$ bands have the same physical circumference momentum of $N = 3, 9$ bands for $N_0 = 6$ case.

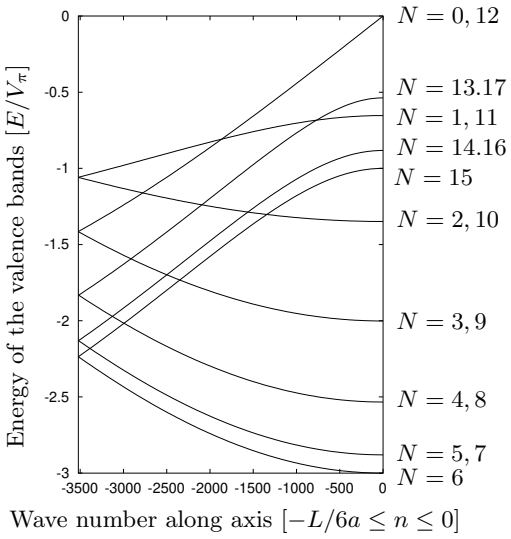

FIG. 1: Negative momentum and energy part of a band structure of the metallic zigzag CNT with $d = 7.04[\mathring{A}](N_0 = 6)$ in diameter. The Fermi energy is set to zero and the horizontal axis denotes wave number. Left most point ($n \approx -3500$) corresponds to $k_y = 2\pi n/L = -\pi/3a$ where L is the length of the zigzag CNT and we take $L = 3[\mu\text{m}]$ in this figure. Each band is labeled by N.

B. Coulomb interaction

The Coulomb interaction between electrons is written by the density of the electron field Ψ_s:

$$\rho = \sum_s \Psi^\dagger_s \Psi_s = \sum_{N,s} \rho_{Ns} + \sum_{N\neq M,s} \rho_{NMs}, \quad (7)$$

where $\rho_{Ns} \equiv \psi^\dagger_{Ns}\psi_{Ns}$ and $\rho_{NMs} \equiv \psi^\dagger_{Ns}\psi_{Ms}$. ρ_{Ns} is a function of the coordinates along tubule axis only but ρ_{NMs} is specified by the position on the surface of CNTs. This is because there is a momentum mismatch along the circumference between ψ_N and ψ_M fields. Therefore it is possible to describe a circumference dependent physical quantity. For example, let us assume that when we put an external charge on a carbon atom the vacuum (ground state) of the system may have an induced charge distribution around it. The induced charge density is described by the vacuum expectation value of the charge density,

$$\langle\rho\rangle = \sum_{N,s}\langle\rho_{Ns}\rangle + \sum_{N\neq M,s}\langle\rho_{NMs}\rangle. \quad (8)$$

The density $\langle\rho_{NMs}\rangle$ may have a non-vanishing amplitude so that it gives the circumference dependence as

$\langle\rho_{NMs}\rangle+\langle\rho_{MNs}\rangle \sim \cos(2(N-M)x/d)$. In this article we consider a circumference independent perturbation and this assumption leads to $\langle\rho_{NMs}\rangle = 0$.

Using the density of the electron field, we define the Coulomb interaction as

$$H_C = \int_S \mathcal{H}_C = \frac{1}{2}\iint_S \rho(r)U(r-r')\rho(r')dr^2dr'^2, \quad (9)$$

where the integral region S denotes the surface of a nanotube and $U(r)$ is the long-range Coulomb potential:

$$U(r-r') = \frac{e^2}{4\pi}\frac{1}{\sqrt{|r-r'|^2+a_z^2}}. \quad (10)$$

$a_z = 1.3[\mathring{A}]$ is a cutoff length which corresponds to the ionization energy ($U(0) = 4V_\pi$) of a π-electron and e is the charge of electron which gives $e^2/4\pi = 1.44[\mathrm{eV}\cdot\mathrm{nm}]$.

Substituting Eq.(7) into Eq.(9), the Coulomb interaction is divided into three blocks:

$$H_C = H_C^a + H_C^b + H_C^c, \quad (11)$$

and each block is given by respectively

$$H_C^a = \frac{1}{2}\iint_S \sum_{N,s}\rho_{Ns}(y)\; U(r-r')\sum_{N',s'}\rho_{N's'}(y')dr^2dr'^2, \quad (12)$$

$$H_C^b = \iint_S \sum_{N,s}\rho_{Ns}(y)\; U(r-r')\sum_{N'M',s'}\rho_{N'M's'}(r')dr^2dr'^2, \quad (13)$$

$$H_C^c = \frac{1}{2}\iint_S \sum_{NM,s}\rho_{NMs}(r)\; U(r-r')\sum_{N'M',s'}\rho_{N'M's'}(r')dr^2dr'^2. \quad (14)$$

In order to get a $1+1$ dimensional model, we have to integrate the circumference degree of freedom. One can perform the integration for H_C^a, and obtain the one-dimensional long-range Coulomb interaction,

$$H_C^a = \frac{1}{2}\iint_D J(y)V(y-y')J(y')dydy', \quad (15)$$

where $V(y)$ is the unscreened Coulomb potential [6]

$$V(y) = \frac{e^2}{4\pi\sqrt{|y|^2+d^2+a_z^2}}\frac{2}{\pi}K\left(\frac{d}{\sqrt{|y|^2+d^2+a_z^2}}\right), \quad (16)$$

with $K(z)$ being the complete elliptic integral of the first kind. The internal density J is defined as the sum of individual fermion densities: $J = \sum_{Ns}\rho_{Ns}$. Here the integral region $S \in [0:\pi d]\times[0:L]$ has changed into $D \in [0:L]$ where L is the length of a nanotube.

Some comments on the one-dimensional long-range Coulomb potential form are in order here. It should be noted that the potential depends on the diameter of CNT. Because of that, one might think, in case of CNTs with large diameter, the Coulomb potential is weak enough to neglect effects of the massive bands on the massless bands. But this is not the case. The band gap of the massive fermions is also scaled as $E_g \equiv V_\pi a/d$, therefore the massive bands may still affect the massless bands for CNTs with large diameter. In fact, the effect of the massive fermions on the massless fermions is universal (it does not strongly depend on the geometry) for any kind of nanotubes. This is shown using a ratio of the potential depth and the gap energy,

$$R \equiv \frac{V(0)}{2E_g} \sim K\left(\frac{d}{\sqrt{d^2+a_z^2}}\right) > 3. \quad (17)$$

The ratio means that when two massless fermions close each other, more than three massive bands come into the dynamics. Specifically, the massive fermions modify the Coulomb interaction between massless fermions. We estimated this effect using one-loop perturbation shortly. In addition, in the case of CNT with large diameter or the multi-walled CNTs, the number of massive fermions also increases so that the correction may be large.

The Fourier mode of the potential is given by

$$\beta_n = \frac{e^2}{2\pi L}\frac{2}{\pi}\int_0^{\frac{\pi}{2}} K_0\left(\frac{2n\pi d}{L}\sqrt{\sin^2 x+\left(\frac{a_z}{d}\right)^2}\right), \quad (18)$$

where K_0 is the modified Bessel function. On the other hand, in some articles [13], the following Fourier component is used

$$v_n = \frac{e^2}{2\pi L}K_0\left(\frac{2n\pi d}{L}\right)I_0\left(\frac{2n\pi d}{L}\right). \quad (19)$$

This correspond to the case of the potential with $\lim_{a_z\to 0}V(x)$. This in turn, would cause an infinite ionization energy of a π-electron. Because of that it is never realistic, especially for large n value. Of course, the Fourier components β_n and v_n for small n value are almost the same, and would be approximated by

$\frac{e^2}{2\pi L}K_0\left(\frac{2n\pi d}{L}\right)$ [14] which corresponds to the following Coulomb potential in coordinate space,

$$V(x) = \frac{e^2}{4\pi}\frac{1}{\sqrt{|x|^2+d^2}}. \tag{20}$$

As for H_C^b, it gives no contribution when one integrate the x and x' circumference coordinates. However H_C^c affect the dynamics in the $1+1$ dimensional system. For example, in the case of $N = M'$ and $M = N'$, the integration can not make the H_C^c term vanish. We calculate the effective Coulomb potential for this case as

$$H_C^c = \frac{1}{2}\iint_D \sum_{N\neq M} J_{NM}(y)V_{NM}(y-y')J_{MN}(y')dydy', \tag{21}$$

where

$$V_{NM}(y) = \frac{e^2}{4\pi\sqrt{|y|^2+d^2+a_z^2}} \times \frac{1}{\pi}\int_0^\pi \frac{\cos 2(N-M)x}{\sqrt{1-\left(\frac{d}{\sqrt{|y|^2+d^2+a_z^2}}\right)^2\cos^2 x}}dx. \tag{22}$$

This potential is short range for $N \neq M$ and weak as compared with the previous Coulomb potential (Eq. 16 corresponds to the $N = M$ case). To see this, we plot these potentials as a function of axis coordinate for a single-wall CNT with typical diameter in Fig. 2.

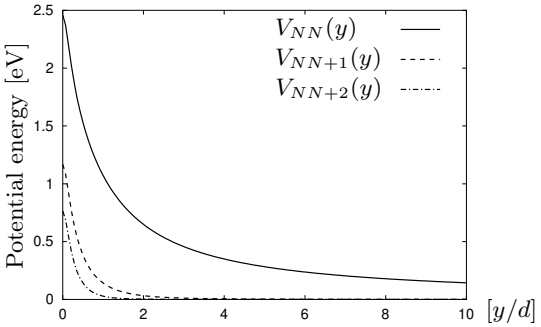

FIG. 2: Coulomb potentials for a CNT with $d = 1.4$[nm] in diameter. The Solid line expresses the potential given in Eq. 16.

Because of the weakness of the interactions in contrast with $V(y)$, we may neglect the interactions for $N \neq M$. Therefore a simple model for π-electrons in CNTs is given by the Hamiltonian

$$H = H_F + H_C^a, \tag{23}$$

where $H_F \equiv \int_D \mathcal{H}_F$. For a tube with huge diameter, we should keep the interactions for $N \neq M$ in a model, however the range of interaction is still short range, so that one may approximate the interaction by an effective point coupling as

$$\begin{aligned}\bar{H}_C^c &\equiv \frac{1}{2}\int_D \sum_{N\neq M} J_{NM}(y)V_{NM}(0)J_{MN}(y)dy \\ &= \sum_{N\neq M}\frac{1}{2}V_{NM}(0)\int_D \rho_{Ns}(y)\rho_{Ms}(y)dy. \end{aligned}\tag{24}$$

In this article we simply use the Hamiltonian (Eq. 23). As a result of this simplification, one can not extent a theoretical result which is obtained from the Hamiltonian Eq. 23 to the CNT with huge diameter simply. Although it is difficult to see the limit of the application of the model Hamiltonian, we think that the model 23 has enough accuracy to describe the π-electrons dynamics in a realistic single-wall CNTs and intralayer interactions in multi-walled CNTs.

In order to study the physics at very low energy scale, it is sufficient to investigate the low energy excitations in the system. Low energy excitations in metallic CNTs are described by a field theory of four massless fermions interacting with each other and with massive fermions through the long-range Coulomb interaction. The massive fermions modify the Coulomb potential between massless fermions because of the vacuum polarization. We will investigate this effect in the following sections.

III. QUANTIZATION OF FERMIONS

We have specified the Hamiltonian that describes the π-electron dynamics in CNTs. In this section we quantize the fermion fields and define propagator of each field. The spin index of the electrons is suppressed in this section for simplicity.

The energy eigenfunctions of the first quantized kinetic Hamiltonian are classified into ψ_N^+ and ψ_N^- that are specified by the energy eigenvalue equations:

$$h_N\psi_N^\pm(k_n) = \pm\Delta_N(k_n)\psi_N^\pm(k_n). \tag{25}$$

ψ_N^+ is the fermion wave function which has a positive energy eigenvalue and ψ_N^- is the one whose energy eigenvalue is a negative value as compared with the Fermi energy. These eigen functions are given by explicitly,

$$\psi_N^\pm(k_n) = \frac{1}{\sqrt{2L}\Delta_N(k_n)}\begin{pmatrix} V_\pi z_N(k_n) \\ \pm\Delta_N(k_n)\end{pmatrix}e^{ik^\pm\cdot r}, \tag{26}$$

where the exponent is defined as $k^\pm\cdot r \equiv \mp\Delta_N(k_n)t/\hbar + k_y^n y$. Here we used the following normalization condition $\int_D \psi_N^{\pm\dagger}\psi_N^\pm dy = 1$ and defined the amplitude $z_N(k_n) \equiv z(k_x^N, k_y^n)$. Because of this definition, the energy eigenvalues leads to

$$\Delta_N(k_n) \equiv V_\pi|z_N(k_n)|. \tag{27}$$

The wave vector along the nanotube axis is quantized by a boundary condition. We take the periodic boundary condition for simplicity and obtain,

$$k_y^n = \frac{2\pi}{L} n \equiv k_n. \tag{28}$$

Using the above eigenfunctions, we construct the quantum fields for the π-electrons as

$$\psi_N = \sum_n \psi_N^+(k_n) a_N(k_n) + \psi_N^-(k_n) b_N^\dagger(k_n). \tag{29}$$

$a_N(k_n), b_N(k_n)$ are independent fermionic annihilation operators of positive and negative energy fermion species labeled by N whose wave vector is k_n and their anticommutation relations are

$$\{a_N(k_n), a_M^\dagger(k_m)\} = \delta_{NM}\delta_{nm}, \tag{30}$$

$$\{b_N(k_n), b_M^\dagger(k_m)\} = \delta_{NM}\delta_{nm}. \tag{31}$$

All of the other anticommutators vanish. The massive mode dynamics is difficult to solve non-perturbative way. Hence we have to use perturbation about the Coulomb charge. To do this, we define a propagator as

$$i\Delta_F^N(x;y) \equiv \langle vac|T\{\psi_N(x)\psi_N^\dagger(y)\}|vac\rangle, \tag{32}$$

where T is the time ordering and the vacuum is defined by

$$a_N(k_n)|vac\rangle = 0, \quad b_N(k_n)|vac\rangle = 0. \tag{33}$$

An alternative representation of the propagator in momentum space is given by

$$\begin{aligned} G_N(E,k_n) &= \frac{1}{E^2 - V_\pi^2 \Delta_N(k_n)^2 + i\epsilon} \\ &\times \begin{pmatrix} E & V_\pi z_N(k_n) \\ V_\pi z_N^*(k_n) & E \end{pmatrix}, \end{aligned} \tag{34}$$

where E is the energy and ϵ is a positive infinitesimal.

IV. VACUUM POLARIZATION

Making use of the propagator of the π-electrons, we compute an amplitude of the vacuum polarization whose Feynman diagram is shown in Fig. 3.
The amplitude for the fermion one-loop diagram is

$$T_n = -\sum_{N,m} \int \frac{dE}{2\pi} \mathrm{Tr}\left[G_N(E,k_m) G_N(E,k_{m-n})\right], \tag{35}$$

where n is an integer and correspond to the wave vector($2\pi n/L$) of the photon. m is also an integer and is an index of the internal fermion wave vector $k_m (= 2\pi m/L)$. N is the band index. The summention of m needs to be restricted within the Brillouin zone, so that

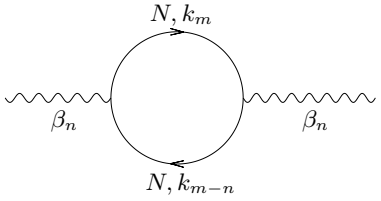

FIG. 3: One-loop vacuum polarization diagram of a π-electron labeled N. β_n is the n-th Fourier component of the unscreened Coulomb potential: $V(x) = \sum_{n\in Z} \beta_n e^{-i2\pi nx/L}$.

it depends on the geometrical structure of CNT. In subsection IV A, we explain region of the summention for a metallic zigzag CNT, as an example.

The vacuum polarization modifies the Coulomb interaction. Fourier components of the modified Coulomb potential are given by

$$\bar{\beta}_n = \frac{\beta_n}{1 - \beta_n T_n}. \tag{36}$$

It should be noted that the amplitude T_n is always an negative value because of the Fermi statistics, so the Coulomb interaction weakens. By performing the energy integration in Eq. 35, we rewrite the one-loop fermion amplitude including the spin degrees as

$$\begin{aligned} T_n &= -\frac{2}{V_\pi} \sum_{N,m} \frac{1}{|z_N(k_m)| + |z_N(k_{m-n})|} \\ &\times \left\{1 - \frac{\mathrm{Re}[z_N(k_m) z_N^*(k_{m-n})]}{|z_N(k_m)||z_N(k_{m-n})|}\right\}. \end{aligned} \tag{37}$$

On the other hand, the vacuum polarization of the massless fermions is calculated exactly using the current algebra supposing that the massless bands are strictly linear bands as

$$T_n = -\frac{8}{\Delta}, \quad n \neq 0, \tag{38}$$

where $\Delta = \frac{3\pi V_\pi a}{L}$ is the single-particle level spacing. This leads to the screened Coulomb potential [14]:

$$\bar{\beta}_n = \frac{\beta_n}{1 + \frac{8\beta_n}{\Delta}} \tag{39}$$

which can be used in a calculation of the induced charge density around an external fixed charge on the surface of the metallic CNTs. The assumption of linear dispersion is thought to be suitable for the metallic zigzag CNT as is shown in Fig. 1. However for the armchair case, the massless bands are not linear for some momentum regions. Hence, we have to check if the vacuum polarization amplitude by the massless fermions loop which is derived from Eq. 37 coincides with the previous estimation [14] of the amplitude derived from the current algebra.

For the metallic zigzag CNTs, there are two massless bands and the hopping amplitude is given by $z_0(k_m) = z_{2N_0}(k_m) = i\frac{3}{2}ak_m$ for all m in the first Brillouin zone with sufficient accuracy. Then one get the same result as Eq. 38,

$$T_n = -\frac{2}{V_\pi}\sum_{0\le m\le n}\frac{2}{|\frac{3}{2}ak_m| + |\frac{3}{2}ak_{m-n}|}\times 2 = -\frac{8}{\Delta}. \quad (40)$$

This is a realization of 'one-loop exact' [15]. As for the armchair CNTs, previous study on the vacuum polarization [13] refer to that there is a logarithmic singularity for a special n of T_n causing the Friedel oscillation. However that is not the case. Because, in order to see such a singularity, the following condition have to satisfy

$$|z_N(k_m)| = |z_N(k_{m-n})| = 0, \quad (41)$$

for some m and n in the Brillouin zone $-\pi/\sqrt{3} \le k_m \le \pi/\sqrt{3}$. For the massless band in the armchair CNTs, the condition $z_N(\pm 2\pi/3\sqrt{3}a) = 0$ holds, then the above condition can not be satisfied for any n in the Brillouin zone. Apart from that, a small cusp structure(not singularity) arises as is shown in Fig. 4. However this cusp due to massless loop is small and is masked by the massive fermion loop amplitude shown in Fig. 5. Therefore the Friedel oscillation around an external charge in (undoped) armchair CNTs will be unobserved. The absence of the Friedel oscillation is supported by a lattice calculation of the screening phenomena [11]. Note also that the result of Eq. 38 for massless fermions is applicable to the armchair CNT with sufficient accuracy. It should be noted that it may be possible to observe some oscillational pattern of an induced charge density around an external charge because of cutting the momentum summention in Eq. 45 [14]. This oscillation has nothing to do with the Friedel oscillation.

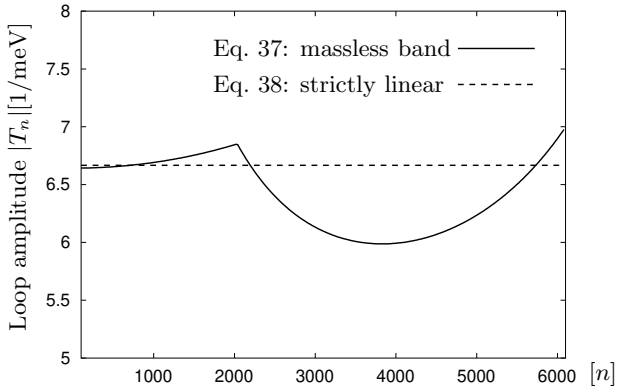

FIG. 4: Absolute value of the loop amplitude $|T_n|$ due to the massless fermions for an armchair CNT with $d = 6.78[\mathring{A}]$ and $L = 3[\mu m]$. The solid line is obtained from Eq. 37 and the dashed line is Eq. 38. One can see that there is a small cusp structure (not singularity).

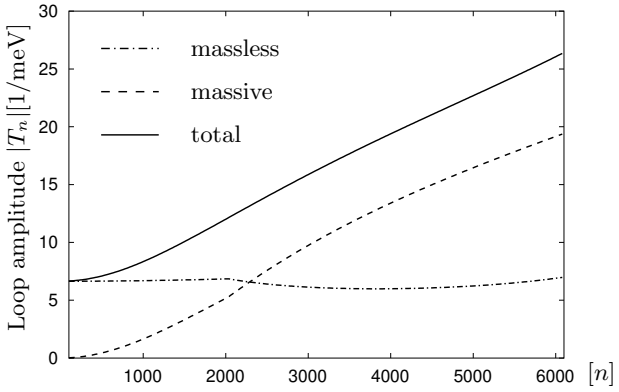

FIG. 5: Comparison between the loop amplitudes due to the massive fermions and massless fermions in an armchair CNT with $d = 6.78[\mathring{A}]$ and $L = 3[\mu m]$. At the wave vector $k_n \sim \mathcal{O}(\frac{\pi}{3\sqrt{3}})$; $(n \approx 2000)$, the effect of the massive fermions exceeds the massless fermions loop amplitude.

In the case of the Coulomb potential is dynamic, that is, has an energy E_n, the corresponding vacuum polarization amplitude is given by

$$T_n(E_n) = -\frac{2}{V_\pi}\sum_{N,m}\frac{|z_N(k_m)| + |z_N(k_{m-n})|}{(|z_N(k_m)| + |z_N(k_{m-n})|)^2 - (E_n/V_\pi)^2} \times\left\{1 - \frac{\mathrm{Re}[z_N(k_m)z_N^*(k_{m-n})]}{|z_N(k_m)||z_N(k_{m-n})|}\right\}. \quad (42)$$

This formula can be used for a study of plasmon excitations, for example.

A. region of the summention

In this subsection, we explain the region of the summention of the loop momentum m in detail. To do so, we first define the phase space of the π-electrons of a metallic zigzag nanotube. Band structure of the π-electrons on the graphite sheet in the momentum coordinate is shown in Fig. 6. The first Brillouin zone is inside the solid square. The horizontal coordinates of the left edge of this square is ak_x^0 and right one is $ak_x^{3N_0}$. Note that these two lines correspond to the same physical state (a massless band). The left edge line $N = 0$ and the dashed line $N = 2N_0$ in the square correspond to the massless bands. Because of the congruent vectors K_1 and K_2 of this space, the wave vector along the axis(y) is restricted to the following region,

$$-\frac{\pi}{3} \le ak_m \le \frac{\pi}{3}. \quad (43)$$

Let us consider a special case of $ak_n = \frac{\pi}{3}, (n = \frac{L}{6a})$ of a photon wave vector. This corresponds to the highest frequency mode of the Coulomb potential. If a massive fermion looping in the diagram have also a large negative momentum $ak_m = -\frac{\pi}{3}(m = -\frac{L}{6a})$, then, there is

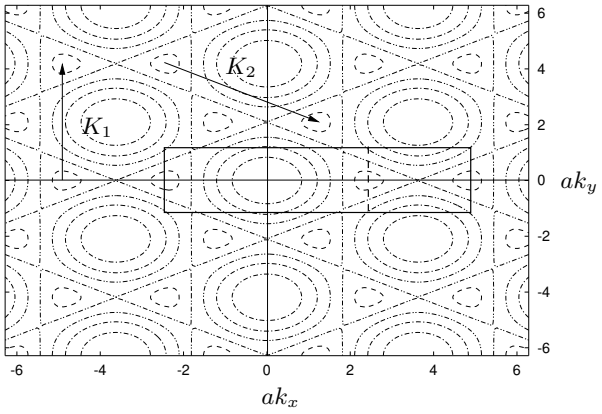

FIG. 6: Band structure of graphite sheet and the first Brillouin zone for a zigzag CNT (inside the solid square).

a fermion in the loop diagram having the wave vector $k_{m-n} = -\frac{L}{3a}$ which is not inside the first Brillouin zone. Therefore we have to back it into the zone. One can do this using the congruent vectors in the space. So, such a fermion having the different wave vector index along circumfernce from the fermion which has the wave vector $k_m = -\frac{L}{6a}$. (Of course, these are the fermions that have the same physical momentum along the circumference as explained before.) This means there is a loop diagram that one fermion belongs to a massive band and the other has a massless band index.

B. numerical estimation

Numerical values of both β_n and $\bar{\beta}_n$ for an armchair CNT with $d = 6.78[\mathring{A}]$ are plotted in Fig. 7. The massive fermions are observed to weaken the Coulomb interaction among the massless and massive fermions as is naturally expected. Because the Coulomb potential is modified by the vacuum polarization effects, the massless fermions interact with each other not via the unscreened Coulomb potential, but via the screened one whose Fourier components are given by $\bar{\beta}_n$. Moreover, in the metallic nanotube, the massless fermions screen the Coulomb interaction too. Hence, real Fourier component of the Coulomb interaction is given by

$$\tilde{\beta}_n = \frac{\bar{\beta}_n}{1 + \frac{8\bar{\beta}_n}{\Delta}} = \frac{\beta_n}{1 - \left[-\frac{8}{\Delta} + T_n\right]\beta_n}, \qquad (44)$$

which is also shown in Fig. 7. The Coulomb interaction in the semiconducting CNTs is screened by the massive fermion loop only. Then, the Fourier components are just $\bar{\beta}_n$. Therefore the Coulomb interaction between massive bands in metallic CNTs has a very weak effective coupling $\tilde{\beta}_n$ but that is not so in the semiconducting CNTs.

We should examine the most effective bands to the vacuum polarization except the massless bands contribution.

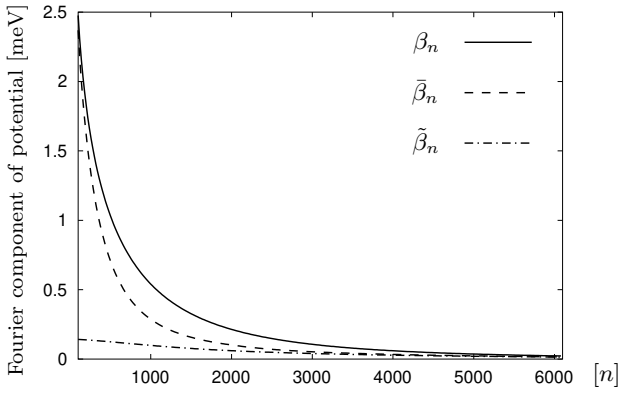

FIG. 7: Fourier component of the unscreened Coulomb potential β_n and the modified one $\bar{\beta}_n$ by the vacuum polarization of the massive bands. We also plot the modified components $\tilde{\beta}_n$ of the Coulomb interaction between π-electrons in metallic nanotube. Here we take the case of an armchair nanotube with $d = 6.78$ [Å] and $L = 3[\mu\text{m}]$.

Naively the most low energy bands except the massless bands would be the one. To check this we plot the amplitude T_n in Fig. 8 including the massive bands labeled N for metallic zigzag CNT and compare it with an amplitude taking into account all the massive bands. From the figure, we can say that the low energy massive bands actually effectively contribute to the total amplitude due to all massive bands, however one should not neglect the effect of the other massive bands.

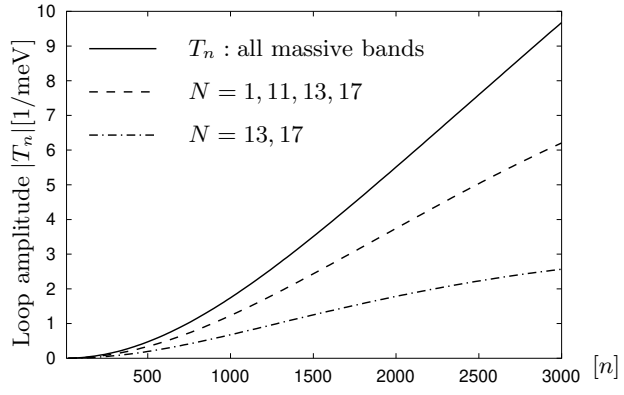

FIG. 8: Absolute value of the loop amplitude $|T_n|$ due to specific massive fermions for a metallic zigzag CNT with $d = 7.04[\mathring{A}]$ and $L = 3[\mu m]$. To understand the definition of the band index N, see Fig. 1.

C. screening

An external charge density can be included by replacing J with $J + J^{ex}$ in the Coulomb interaction (Eq. 15), where J^{ex} is a c-number whose integral over the nanotube

length is equal to the total external charge. Here we take a point external charge distribution which is modeled by $J^{ex} = \delta(x - x_0)$ where x_0 is the position of the external charge along the tubule axis. The configuration of the external charge has symmetry around the circumference of a tube. In Fig. 9 and Fig. 10, the induced charge distributions around the external point charge for both armchair and metallic zigzag CNT are depicted. These are obtained using the following formula [14, 16]

$$\langle J(x)\rangle = \sum_{n>0} -\frac{\frac{8\bar{\beta}_n}{\Delta}}{1+\frac{8\bar{\beta}_n}{\Delta}}\frac{2}{L}\cos\left(\frac{2\pi n}{L}(x-x_0)\right). \quad (45)$$

It should be noted that the screening length is about the diameter of the nanotube [14] for both cases and is not sensitive to the length of the nanotube. Note also that there is a oscillation in the induced charge density around the external charge and this is not the Friedel oscillation as already mentioned.

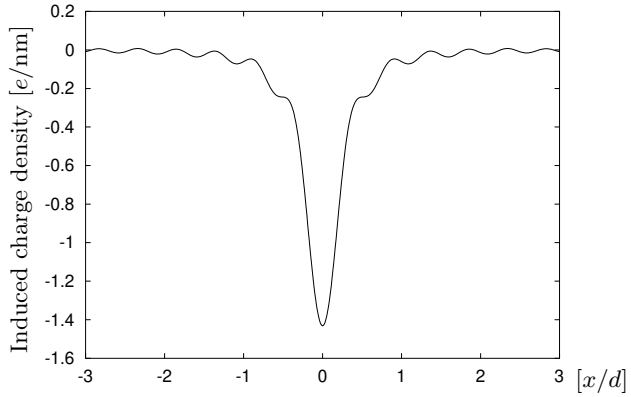

FIG. 9: Induced charge density (including spin degeneracy) along the nanotube axis for armchair CNT with $d = 6.78[\mathring{A}]$ and $L = 3[\mu m]$. An external unit charge locates at the origin.

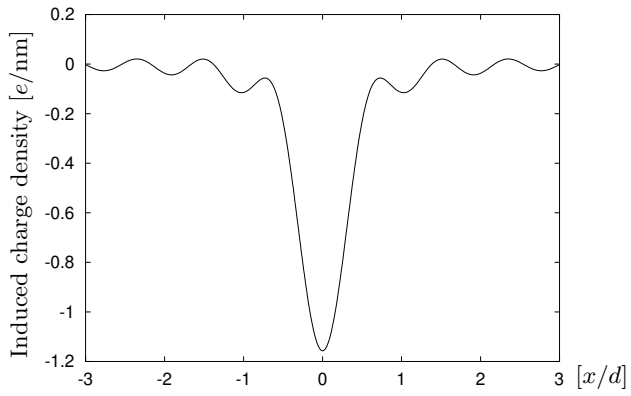

FIG. 10: Induced charge density (including spin degeneracy) along the nanotube axis for metallic zigzag CNT with $d = 7.04[\mathring{A}]$ and $L = 3[\mu m]$. An external unit charge locates at the origin.

V. SUMMARY AND DISCUSSION

In summary, we have constructed a field theoretical model of the π-electrons in metallic and semiconducting CNTs and calculated the vacuum polarization amplitude for several single-wall CNTs at one-loop level. The massive and massless bands are shown to have decisive role in the spectrum of the Coulomb interaction in nanotubes, through the modification of the Coulomb potential by the vacuum polarization. We also found that the absence of the Friedel oscillation in the screening phenomena which is due to the phase space constraint of the electron momentum along nanotube axis.

We mention the relationship between our results and the previously published article studying effects of the massive bands. M.F. Lin and D.S. Chuu [13] are the first who concern the effect of the massive bands on impurity screening; vacuum polarization. Several results in their paper are incorrect. First, they defined the response function(T_n in the present article) as a positive value which must be a negative value. Second they pointed out that there is strong short-wavelength Friedel oscillation in armchair CNTs. However this is not the case, because of the momentum constraint in CNTs. We make sure that the screening length is sensitive to the diameter of metallic nanotubes with small diameter. This fact would not be applicable to the nanotube with huge diameter because it is shown by a lattice calculation that non-perturbative effects of the massive bands on screening is strong [11]

Finally we would like to discuss the vacuum polarization effect in multi-walled CNTs. The number of the massive bands increase as the diameter become thick and the gap energy decreases at the same time. Therefore it is naturally expected the vacuum polarization correction on the long wave length modes of the Coulomb interaction is large. This may causes the modification of the low energy effective theory of the multi-walled CNTs.

[1] S. Iijima, Nature, **354**, 56 (1991).
[2] C. Dekker, Phys. Today **52**, No. 5, 22 (1999).
[3] J. W. G. Wildöer et al., Nature, **391**, 59 (1998); T. W. Odom et al., Nature, **391**, 62 (1998).

[4] C.L. Kane and E.J. Mele, Phys. Rev. Lett. **78**, 1932 (1997).
[5] C. Kane, L. Balents and M.P.A. Fisher, Phys. Rev. Lett. **79**, 5086 (1997).
[6] R. Egger and A. O. Gogolin, Phys. Rev. Lett. **79**, 5082 (1997); Eur. Phys. J. B **3**, 281 (1998).
[7] H. Yoshioka and A.A. Odintsov, Phys. Rev. Lett. **82**, 374 (1999).
[8] S.J. Tans et al., Nature (London) **386**, 474 (1997); S.J. Tans et al., Nature (London) **394**, 761 (1998); H. Postma et al., J. Low. Temp. Phys. **118**, 495 (2000).
[9] M. Bockrath et al., Nature (London) **397**, 598 (1999); H.Postoma et al., Science **293**, 76 (2001).
[10] A.A. Farajian, K. Esfarjani and M. Mikami, Phys. Rev. B **65**, 165415 (2002).
[11] K. Sasaki et al., arXiv:cond-mat/0205637.
[12] The definitions of subscripts $\bullet$ and $\circ$ in Eq. 1 and the vector u_i in Eq. 5 are found in the following articles: K. Sasaki, Phys. Lett. A **296**, 237 (2002); K. Sasaki, Phys. Rev. B **65**, 155429 (2002).
[13] M.F. Lin and D.S. Chuu, Phys. Rev. B **56**, 4996 (1997).
[14] K. Sasaki, Phys. Rev. B **65**, 195412 (2002).
[15] J. Schwinger, Phys. Rev. **128**, 2425 (1962).
[16] We have to specify the cutoff of n in the vacuum expectation value of the internal density. We set it $\frac{1}{2\sqrt{3}}\frac{L}{a}$ for the armchair CNT. This cutoff causes an oscillatory pattern [14] of the induced charge density for the Coulomb interaction in the text.